

# PERSISTENT 1.5 s OSCILLATIONS SUPERIMPOSED TO A SOLAR BURST OBSERVED AT TWO mm-WAVELENGTHS

A. M. ZODI and P. KAUFMANN

*INPE: Instituto de Pesquisas Espaciais, CNPq, Caixa Postal 515, 12.200-São José dos Campos, SP, Brazil*  
and

H. ZIRIN

*Big Bear Observatory, California Institute of Technology, Pasadena, CA 91125, U.S.A.*

(Received 31 May, 1983; in revised form 2 February, 1984)

**Abstract.** Long-enduring quasi-periodic oscillations (1.5 s) superimposed upon a solar burst have for the first time been observed simultaneously at two different mm-wavelengths (22 GHz and 44 GHz). The oscillations were present throughout the burst duration (about 10 min), and were delayed at 44 GHz with respect to 22 GHz by 0.3 s. The relative amplitude of the oscillation was of about 20% at 44 GHz and of about 5% at 22 GHz. Interferometer measurements at 10.6 GHz indicated the burst source position stable within 1 arc sec. An He I D<sub>3</sub> line flare showed two persistent small spots separated by about 10 arc sec. The 22/44 GHz burst position corresponds well with the location of the He I D<sub>3</sub> spots. The oscillations display features which distinguish them from ultrafast time structures found in other bursts. One possible interpretation is a modulation of the synchrotron emission of trapped electrons by a variable magnetic field on a double burst source, optically thin at 44 GHz and with optical thickness  $\lesssim 0.3$  at 22 GHz.

## 1. Introduction

Pulsations superimposed to microwave solar bursts were known for a long time (Janssens and White, 1969; Janssens *et al.*, 1973; Maxwell and Fitzwilliam, 1973; Kaufmann *et al.*, 1977; Urpo *et al.*, 1981). Some bursts were observed simultaneously at more than one frequency, but with low sensitivity and poor time resolution. In this paper we present observations obtained with high sensitivity and time resolution at Itapetinga Radio Observatory. Persistent quasi-periodic oscillations (period  $\sim 1.5$  s) have been observed at two mm-microwaves (22 GHz and 44 GHz) and a time delay of 0.3 s was determined for the pulses at 44 GHz with respect to those at 22 GHz. The oscillations were observed throughout the entire radio burst duration (of about 10 min). The 10.6 GHz burst data from Owens Valley Radio Observatory (OVRO) interferometer provided position information. At optical wavelengths, the flare was analysed using data from Big Bear Observatory. This burst corresponded to a flare which occurred on 15 December, 1980 at region 2840 (NOAA number) covering the period 19:18–19:52 UT, at heliographic position N11 E28 (NOAA, 1981a).

The quasi-periodic pulsations associated with microwave solar bursts may be separated into various categories; the most commonly observed one consists in chains with few pulses (not more than few tens), separated by nearly regular time intervals. A classical example has been analysed by Parks and Winckler (1969). Another and different class consists of long-enduring, uniform oscillations which persist throughout

the event duration (Kaufmann *et al.*, 1977). The first class may represent a succession of bursts independent from each other while the second class may correspond to modulation of the burst radiation.

A third kind of pulsation correspond to the ultrafast structures detected in superposition of mm-microwave bursts, with repetition rates (or quasi-periodicity) varying with the underlying flux level (Kaufmann *et al.*, 1980).

The oscillations studied here pertain to the second class, with quasi-periodicity as well as a phase difference persisting about the same along almost 10 min.

We suggest that the regularity of the pulsations may be explained in terms of the modulation mechanism described below, which considers the emission arising from two sources lying close to the footpoints of a slightly asymmetric magnetic loop. The phase difference of the oscillations at different frequencies can be attributed to the influence of the optical thickness at the source. It was discussed in limiting cases (i.e., optically thin and thick) by Gotwols (1973) and by Gaizauskas and Tapping (1980). The assumption of asymmetrical magnetic loops has been used to explain polarization features of solar microwave bursts (Kundu and Vlahos, 1979; Kosugi, 1981).

## 2. Description of the Instrumentation

The burst studied in this paper was recorded using the 45 ft radome-enclosed antenna at Itapetinga Radio Observatory. The general characteristics of the antenna and its application to solar radio-astronomy was described elsewhere (Kaufmann *et al.*, 1982a). For the present application antenna feed consisted of a single linearly polarized horn with 22 GHz and 44 GHz outputs. The sensitivity in terms of solar flux units ( $1 \text{ s.f.u.} = 10^{-22} \text{ W m}^{-2} \text{ Hz}^{-1}$ ) was of about 0.03 s.f.u. r.m.s., for a time constant of 1 ms for sources sufficiently small compared to the antenna beam-width respectively 4 arc min and 2 arc min at 22 GHz and 44 GHz. The tracking accuracy was better than 2 arc sec r.m.s. Spatial displacements of hot spots are determined either by mapping, or by moving the antenna coordinate controls. The accuracy in the determination of spatial positions and displacements depend on the strength of the hot spots compared with the background; it can be as good as 10 arc sec.

## 3. Observational Characteristics at Microwaves

The entire 15 December, 1980 burst, as observed at Itapetinga, is shown in Figure 1. It can be subdivided into two events. Although both were associated to the same optical flare, the two bursts have distinct characteristics.

The burst labeled (A) started at about 19:20 UT, in association with the impulsive phase of the H $\alpha$  flare. The second burst started at about 19:28 UT, before the level of the first burst returned to normal. The second burst has an entire duration of about 10 min with a peak at about 19:31 UT. The 1.5 s oscillations were observed during the second burst. Radio data obtained at other frequencies (NOAA, 1981b) indicate that event (A) has a spectrum maximum at the lower microwave frequencies, while the

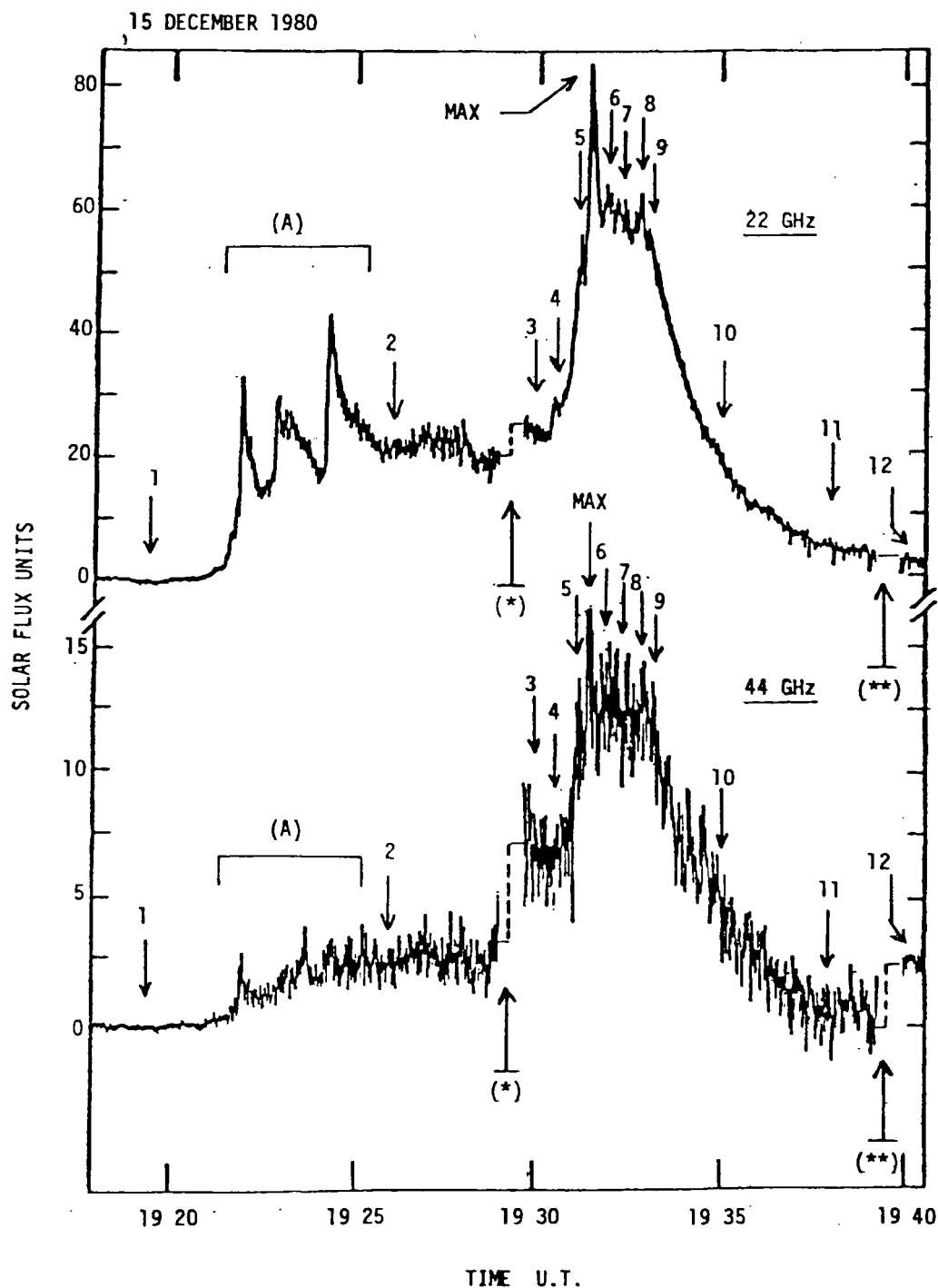


Fig. 1. The 15 December, 1980 burst as observed at Itapetinga Observatory at 22 GHz (top) and 44 GHz (bottom). The persistent 1.5 s oscillations were observed for the second burst, becoming pronounced after the first pointing correction (for maximum signal) at 19:29 UT, labeled (\*). Another pointing correction was made at 19:39 UT, labeled (\*\*). Arrows, labeled by numbers, indicate 10 s sections which are shown expanded in Figure 2(a) and (b).

second event emission was stronger for higher frequencies. Another distinction between the two bursts is that in burst (A), analysed separately (Kaufmann *et al.*, 1982b), there were no quasi-periodicities and no correlation between time structures at the two frequencies.

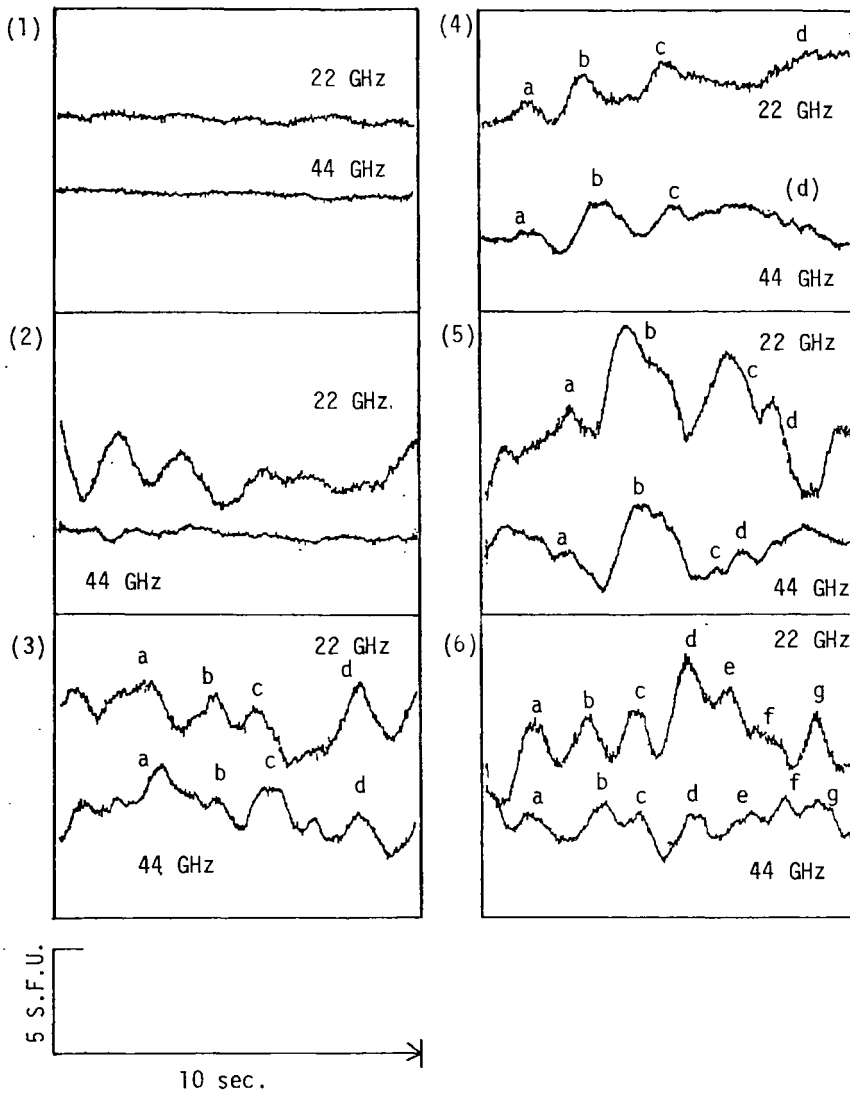


Fig. 2a.

Fig. 2. 10 s samples taken across the burst shown in compressed time scale in Figure 1, at the times indicated by the arrows with correspondent label number. Flux scale is the same for all sample-sections, for both frequencies, and is indicated at the bottom left corner. Identified time structures corresponding to each other are labeled by letters.

In association to burst (A) a type V event was reported from 19:22.8 UT to 19:23.9 UT (NOAA, 1981a), suggesting that there were energetic electrons trapped in a closed magnetic field.

We have labeled the burst sections in Figure 1 by arrows from 1–12, which were expanded into 10 s samples, displayed in Figure 2(a) and 2(b). The flux scale is the same for all sections and is shown in the bottom of Figure 2(a) and 2(b).

Two pointing corrections were made, orienting the antenna beam at the emission maximum position at 19:29 UT, label (\*) and at 19:39 UT, label (\*\*), as indicated by dashed lines in Figure 1.

The following characteristics are found in Figures 1 and 2(a) and 2(b):

(i) A quasi-periodicity is clearly present at both frequencies, from section (3), at the

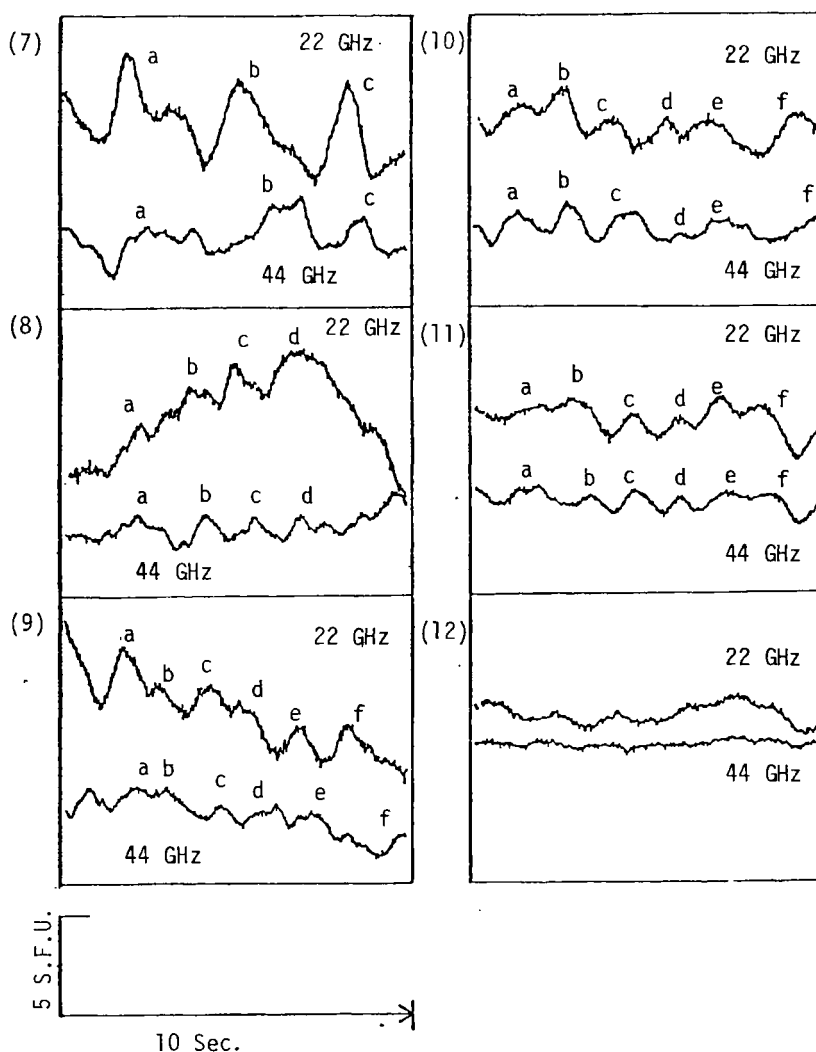


Fig. 2b.

beginning of the second burst, through section (11). There are 4–7 pulses per 10 s section.

(ii) Although sometime the correlation is not so good between the two frequencies, for most of the 10 s sections there is a nearly one-to-one correspondence between the structures as labelled by letters. In these cases, the 44 GHz pulses appear delayed with respect to the 22 GHz pulses.

(iii) Before the burst (section (1)) there are no oscillations with amplitude larger than 0.2 s.f.u. at 22 GHz and 0.15 s.f.u. at 44 GHz, when tracking AR2840. After the burst (section (12)), and with the antenna displaced to the maximum emission position, the oscillation amplitude is again reduced at 22 GHz and 44 GHz (to less than 0.5 s.f.u. and 0.2 s.f.u., respectively). After burst (A) and before second burst (section (2)), an oscillation is observed at 22 GHz (with amplitude of about 2 s.f.u.), but is about ten times smaller at 44 GHz. Correlated emission at the two frequencies appear when the antenna was pointed to the maximum emission position corresponding to the second burst.

(iv) The amplitude of the oscillations rises as the second burst flux level rises.

(v) The fluxes at 22 GHz ( $S_{22}$ ) and at 44 GHz ( $S_{44}$ ) have the approximate relationship  $S_{44} \approx S_{22}/5$ . The amplitudes of the oscillations,  $\Delta S_{22}$  and  $\Delta S_{44}$ , respectively, are comparable, for different flux levels, such that the relative importance of the quasi-periodic pulsations are of about  $(\Delta S_{22}/S_{22}) \approx 5\%$  and of  $(\Delta S_{44}/S_{44}) \approx 20\%$ . According to this trend, at 10.6 GHz the relative amplitude would be close to one percent, and indeed they were not detectable in OVRO data.

The quasi-periodicity and the phase delay are better shown in Figure 3, where we show the result of a cross-correlation of the two 22 GHz and 44 GHz signals taken from 19:30–19:35 UT. This was obtained with the use of a correlator (HP 3721A), in AC mode. The scale of cross-correlation coefficients was left in arbitrary units because the correlator response for frequencies smaller than 1 Hz was not linear. The result in Figure 3, however, is qualitatively very significant. It confirms the results from the previous inspection of Figure 2(a) and 2(b). The plot in Figure 3 indicates maxima in the relative cross-correlation coefficients, separated by 1.5 s (the quasi-periodicity common to both signals), and the delay of 0.3 s of 44 GHz with respect to 22 GHz.

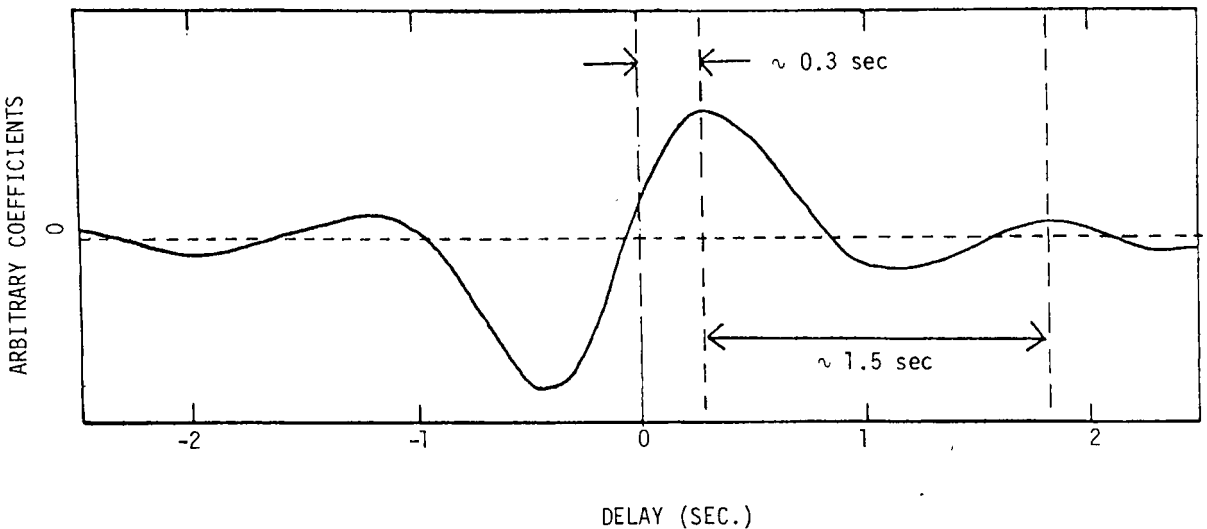


Fig. 3. Cross-correlation of 22 GHz and 44 GHz burst emission, taken in the time interval 19:30–19:35 UT, and covering the principal rise and fall phase of the event. Cross-correlation coefficients are in arbitrary units. The 1.5 s quasi-periodicity and the 0.3 s delay of 44 GHz oscillations (relative to 22 GHz), are indicated.

The spatial positions for which maximum emission was obtained at 22 GHz and 44 GHz are shown in Figure 4. Position 1 is for the region nearly 30 min before the burst occurred. The half-intensity contours were obtained from a map taken earlier in the day (continuous for 22 GHz and dashed for 44 GHz). As the burst developed, an antenna pointing adjustment was made at 19:29 UT (labeled by \* in Figure 1); the maximum emission was then located at position 2, at about 1.5 arc min away from position 1 and closer to the neutral line. After the burst decay, at 19:39 UT, another adjustment was made (labeled by \*\* in Figure 1). The maximum radio emission was at position 3, more than 1 arc min from positions 2 and 1, and again east from the neutral line. Although

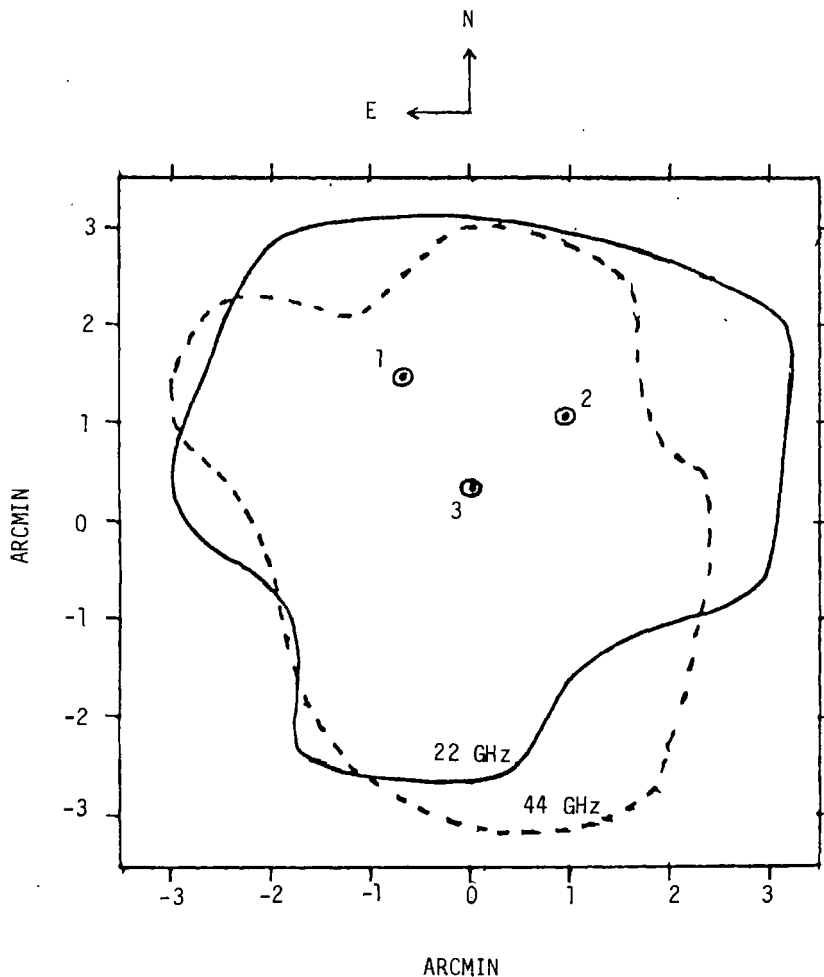


Fig. 4. The microwave radio maximum positions: (1) 30 min before the burst, (2) after pointing adjustment at 19:29 UT, and (3) after pointing adjustment at 19:39 UT. The half-power radio contours of the active region correspond to the map obtained earlier in the day centered at N09 E32. The half-power active region sizes are comparable, and larger than the half-power beamwidths at 22 GHz (4 arc min) and at 44 GHz (2 arc min), indicating that the preburst region was extended or made up by several spots across the antenna beams.

the radio-emission was higher at position 3, the oscillation was only present at position 2 (see Figure 2(b), sections (11) and (12)). This suggests that the oscillatory phenomena was associated specifically with position 2, and not involving other positions within the active region.

#### 4. Observational Characteristics at Optical Wavelengths

The active region had a strongly sheared neutral line between two rows of sunspots; but the flare described occurred near some rapidly changing smaller spots nearby which formed a peninsula of following polarity surrounded by preceding polarity.

The flare event began with a filament lifting at 19:15 UT. The optical flare showed two distinct components corresponding to the radio event. There was an impulsive flash at 19:21:04 UT (the first detectable optical increase was at 19:18 UT). Figure 5 shows

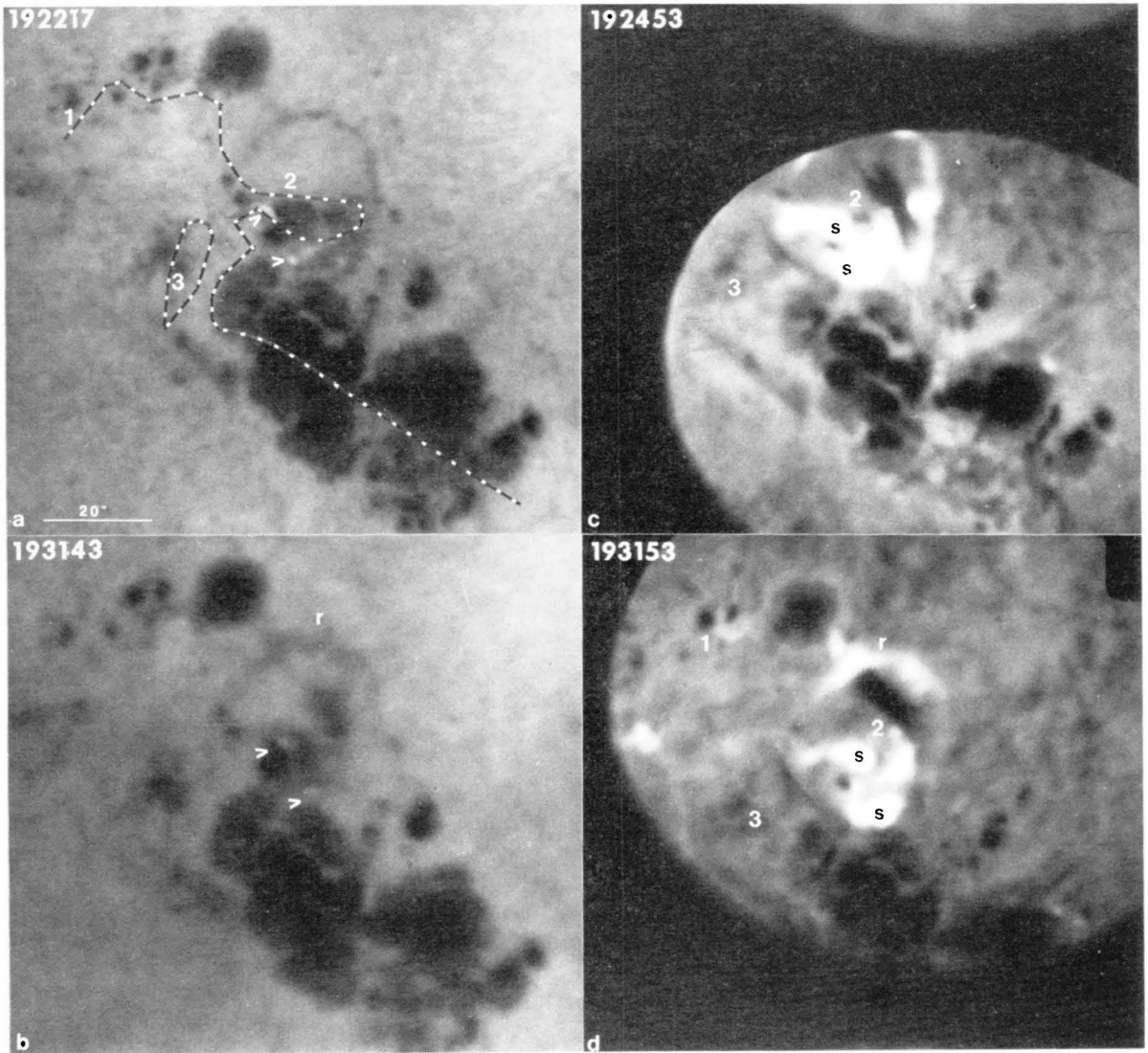


Fig. 5. Frames of the flare in He I  $D_3$  (left) and  $H\alpha - 0.7 \text{ \AA}$  (right). North is up and east, left. The kernels of  $D_3$  emission are marked by arrows. The most intense  $H\alpha$  kernels are marked 's' in (c) and (d), and the rim of  $H\alpha$  emission and  $D_3$  absorption is marked  $r$ . The numbers 1, 2, and 3 correspond to the locations of the radio sources mentioned in the text. The longitudinal neutral line of magnetic field is marked. One sees how the flare occurred on an inclusion of  $f$  polarity. The position change between kernels of the first and second event is small, less than 10 arc sec.

the flare in  $D_3$  and  $H\alpha$  both during the impulsive phase and the late microwave peak. Arrows mark the two  $D_3$  footpoints, and the positions of the microwave sources 1, 2, and 3 (referred to Figure 4) are also marked. A line indicates the approximate neutral line from videomagnetograms. A bright rim of emission ( $r$ ) was matched by a dark  $D_3$  absorption rim. This rim corresponds to the nearest area of  $p$  polarity. The bright  $D_3$  footpoints were separated by 10 arc sec, and one would expect the microwave source to be between them. There was dark ejecta. The peak of  $D_3$  emission was 19:24 UT and 19:27 UT. A dark surge appeared at 19:24 UT which moved in front of the rim.

The optical event at the time of the microwave peak at 19:30 UT was weak, but correspond to a resurgence in the optical activity. In  $D_3$  there was renewed brightening and two footpoints rapidly moved 5 arc sec from E to W between 19:29 and 19:31 UT;

then motion ceased. There was rapid motion and change. In  $H\alpha$  an extremely bright single kernel appeared at one of the footpoints. This 'third kernel' was found by Zirin and Neidig (1981) and Feldman *et al.* (1983) in other events; it is typical in late peaks of flare intensity. There was also some change in the rim  $r$ . There is really nothing in the optical data to suggest the greater strength of the microwave peak at the time of oscillations.

Although a dark surge and  $D_3$  absorption moved across the rim  $r$  during the entire period 19:29–19:36 UT, a dark filament between  $r$  and the kernels was not disturbed nor did the emission from  $r$  change.

Considering the errors of position measurements made with a single antenna, the microwave location of source 2 within 10 arc sec of the midpoint of the optical kernels is good. Whether the coincidence of source 3 with another inclusion is significant cannot be determined.

### 5. Discussion of the Observation Results

Oscillations like those observed can be caused by various processes, some instrumental and some not. The pulsations could be produced by antenna beam oscillations across a fixed burst source. This possibility can be ruled out for the following reasons: (a) in order to produce amplitude fluctuations up to 30% (as observed at 44 GHz) the antenna beam would have to be displaced by about 1 arc min, which is much larger than the actual tracking accuracy (better than 2 arc sec) or than the spatial positioning accuracy (over the peak radio emission, about 10 arc sec). (b) When the antenna pointing adjustments were made (Figure 1, label \*) the amplitude of oscillations increased as the pointing errors were reduced, instead of decreasing as would be expected from an instrumental effect, i.e., for an oscillating antenna beam, the amplitude of observed oscillation is larger when the tracking of the peak emission point source is offsetted. (c) Burst (A) should have shown the same kind of oscillation, which it did not (Kaufmann *et al.*, 1982b).

Another possibility could be a quasi-periodic movement of the source across the beam (or different sources turning on and off at different spatial positions). This, however, do not seem to have been the case, since: (a) the maximization of peak burst position (label \* in Figure 1) would not be possible for source displacements of the order of 1 arc min. (b) Such displacements, if present, would not give plausible values for the source velocity ( $\sim 3 \times 10^4$  km s<sup>-1</sup>). (c) Radio interferometric observation of the same burst at 10.6 GHz at Owens Valley Radio Observatory has shown the phase of the correlated signals from the two antennas remained stable from 19:30–19:35 UT, indicating that the radio source was stationary within 1 arc sec, in one dimension (quasi-periodicities, with amplitude larger than the sensitivity of the data display of 0.5 s.f.u., or one percent, were not found at 10.6 GHz). (d) Big Bear Solar Observatory observations of the He I  $D_3$  line flare show two small regions, separated by about 10 arc sec, remaining in the same position during the second burst. The rapid movement of the two  $D_3$  footpoints by 5 arc sec, from 19:29–19:21 UT (described in the previous section) had no corre-

spondence on OVRO interferometer data at 10.6 GHz, where the radio source remained stable within 1 arc sec. At Itapetinga a displacement of 5 arc sec is not detectable.

Finally, the influence of tropospheric propagation on the oscillations can also be ruled out since observations of this burst at Itapetinga were carried out under clear sky conditions. Furthermore, the phase difference between 22 GHz and 44 GHz could not be explained by atmospheric effects. A discussion on possible observational effects and limitations has been given elsewhere (Kaufmann *et al.*, 1984). Therefore, the evidence supports the assumption that the oscillations originated in the emitting region, remaining stationary and aligned with the antenna beam axis, at position 2 of Figures 4 and 5.

## 6. Interpretation

The suggested interpretation of the persistent quasi-periodic oscillations superimposed to a solar burst emission at mm-microwaves was carried out taking into account the following summary of the observational evidence: the oscillations displayed had a dominant quasi-period of 1.5 s, and were persistent over about 10 min. They were noticed even before the rise of the second burst. The oscillations appeared after the occurrence of a metric type V burst. Simultaneous observations at more than one frequency indicated the 44 GHz structures delayed by 0.3 s with respect to 22 GHz. This delay remained significantly the same for all sections analysed throughout the burst duration.

The uniformity of the phenomenon suggest the existence of a physical agent which produce a regular modulation of the emission. We think that other transient effects or random processes would produce changes in time of the observed characteristics. On the other hand, the occurrence of a type V burst in the first burst justifies the assumption that part of the electrons accelerated were trapped in the magnetic structure and, therefore, that their emission could be modulated by MHD instabilities.

There are few models available for the interpretation of oscillations superimposed to solar bursts. The suggested interpretations require some basic assumptions such as modulation of emission by waves (Chiu, 1970; Gotwols, 1973; Tapping, 1978); quasi-periodic acceleration of electrons or successive occurrence of elementary explosions (Urpo *et al.*, 1981; Emslie *et al.*, 1981; Brown *et al.*, 1983). Some models associate the modulation of emission with the oscillation of the magnetic field on the region (Gaizauskas and Tapping, 1980). This possibility appear to be more consistent with the regularity of the observed characteristics. We will therefore assume that magnetic field oscillations modulate the synchrotron emission of the energetic electrons produced in the flare and trapped in a bipolar magnetic structure.

MHD oscillations can arise in density enhancements like coronal loops and can be trapped in these magnetic flux tubes. Spruit (1982) has analysed the wave modes in a slender flux tube, namely, a tube of radius much smaller than the wavelength along the field lines, and found three types of tube wave: a torsional Alfvén wave, an asymmetrical (kink) wave and a symmetrical (sausage) wave. The first two have Alfvénic speeds and the last one propagates with slow velocity (of the order of the sound speed). Roberts

*et al.* (1983, 1984) extended the analysis for shorter wavelengths and derived the characteristic speeds of free modes in the coronal tube, considering standing and propagating oscillations. In this more general assumption, both the asymmetrical and the symmetrical wave can have acoustic (slow mode) or Alfvénic (fast mode) time scales. The fast modes are dispersive and the symmetrical oscillations have the shortest periods in the system.

In our analysis we are considering time-variation of magnetic field strength, which involve compressive tube wave. However, the modulation of synchrotron emission by non-compressive torsional Alfvén waves can produce similar effects and the modulation is produced by changing the magnetic field direction with respect to the observer (Tapping, 1983).

We consider that the electrons have a isotropic power law energy distribution, with index  $\gamma$ :

$$N(E) = N_0 E^{-\gamma}.$$

The intensity emitted at the frequency  $\nu$  by a volume of thickness  $s$ , with an uniform magnetic field, is the well-known equation of radiative transfer:

$$I_\nu = S_\nu(1 - e^{-\tau_\nu}) \quad (1)$$

with  $S_\nu = \varepsilon_\nu/\kappa_\nu$ , and  $\tau_\nu = \kappa_\nu s$ , where  $\varepsilon_\nu$  is the emissivity and  $\kappa_\nu$  is the coefficient of synchrotron self-absorption. We shall assume that both  $\varepsilon_\nu$  and  $\kappa_\nu$  are constant across the source.

In order to justify the phase difference between the oscillations at the two observed frequencies, we will assume that the emission arises from a double source (see Figure 6), close to the footpoints of a bipolar magnetic structure, with the magnetic field strength slightly different at the two ends. A magnetic disturbance originates at some point in the structure (indicated by  $\times$  in Figure 6). It propagates along the field lines at velocity of the order of the Alfvén speed, reaching the two emitting regions at different phases

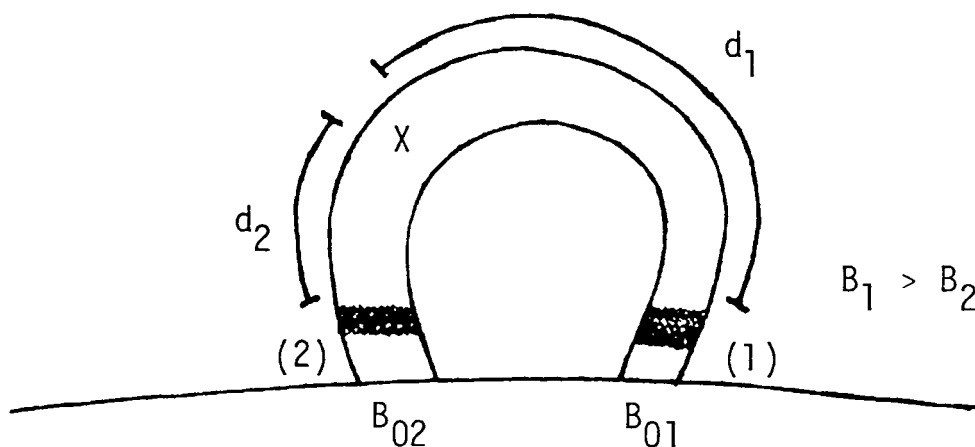


Fig. 6. Simplified diagram showing one asymmetric magnetic arch and a possible location of the agent of magnetic field modulation. The perturbation originate at the  $\times$  point, reaching the two sources located at distances  $d_1$  and  $d_2$ . Sources (1) and (2) are tentatively associated to He I  $D_3$  footpoints indicated by arrows in Figure 5.

of the cycle, depending on the distance of from the two regions. The combined emission from the two regions will produce a phase difference between the time structures at frequencies for which the sources having significantly different optical thicknesses.

Using simplified equations for the emissivity and synchrotron self-absorption coefficient, in the relativistic limit (Pacholczyk, 1970), we have:

$$\varepsilon_\nu \sim N_0 (B \sin \psi)^{(\gamma+1)/2} \nu^{-[(\gamma-1)/2]}, \quad (2)$$

$$\kappa_\nu \sim N_0 (B \sin \psi)^{(\gamma+2)/2} \nu^{-[(\gamma+4)/2]}, \quad (3)$$

where  $B$  is the magnetic field, and  $\psi$  is the angle between the direction of  $B$  and the observer. These equations are valid for ultra-relativistic electrons with an isotropic pitch angle distribution. At footpoints this assumption do not represent a strictly realistic description. The simplifications, however, are often adopted in the litterature in order to permit the obtention of quantitative results to compare with observations.

Assuming that the number and energy distributions of energetic electrons are the same at both sources, and that their physical thickness are comparable, we have

$$\frac{S_2}{S_1} \simeq \left( \frac{B_1}{B_2} \right)^{0.5}, \quad (4)$$

$$\frac{\tau_1}{\tau_2} \simeq \left( \frac{B_1}{B_2} \right)^{(\gamma+2)/2},$$

where we have also assumed that  $\psi_1 \approx \psi_2$ , which is reasonable for small wave amplitudes.

The total intensity from the two sources (1 and 2) will be

$$I = S_1 + S_2 - (S_1 e^{-\tau_1} + S_2 e^{-\tau_2}). \quad (5)$$

It is convenient to express the resulting intensity, given by Equation (5), in the form of Equation (1), where

$$S = S_1 + S_2 \quad \text{and} \quad e^{-\tau} = (S_1 e^{-\tau_1} + S_2 e^{-\tau_2}) / (S_1 + S_2). \quad (6)$$

Adding a subscript 0 for the undisturbed state, designating  $A = B_{01}/B_{02}$ , we can obtain a relationship between the undisturbed mean value for  $\tau_0$ , according to Equation (6), and  $\tau_{01}$  with use of Equation (4):

$$A^{0.5} \exp[-A^{-[(\gamma+2)/2]} \tau_{01}] + e^{-\tau_{01}} = (1 + A^{0.5}) e^{-\tau_0}. \quad (7)$$

Expressing the oscillation of  $B$  in the simplest case of a sinusoidal variation, for small wave amplitudes we have:

$$B_1 = B_{01}(1 + K_1 \sin \omega t), \quad (8)$$

$$B_2 = B_{02}[1 + K_2 \sin(\omega t + \phi)],$$

where  $\phi$  is the phase difference between oscillations of  $B$  at the regions 1 and 2, and  $K_1$  and  $K_2$  are the amplitudes of the variations of  $B_1$  and  $B_2$ .

If there is conservation of the flux of magnetic energy of the wave along the loop, the amplitudes  $K_1$  and  $K_2$  are related as follows:

$$\frac{K_2}{K_1} \approx \sqrt{\frac{n_2}{n_1}} A^3, \quad (9)$$

where  $n_{1,2}$  are the electron densities in the media.

The phase difference between the time structures at two frequencies  $\nu$  and  $\nu'$  is calculated by  $\Delta t = t_{m\nu} - t_{m\nu'}$ , where  $t_{m\nu}$  and  $t_{m\nu'}$  are the times of maxima of  $I_\nu$  and  $I_{\nu'}$ .

The flux densities observed at the peak of the second event were 106 s.f.u. and 110 s.f.u. for 9.4 GHz and 15.4 GHz, respectively (NOAA, 1981b), and of about 80 s.f.u. and 16 s.f.u. at 22 GHz and 44 GHz, respectively. These values suggest a spectral maximum at a frequency around 15 GHz. The flux densities at 22 GHz and 44 GHz provide a  $\gamma \approx 5$ .

In Figure 7 we plotted the phase difference relative to the period  $p$  of oscillation ( $\Delta t/p$ ) with the optical depth  $\tau_0$ , for three values of  $A$ . We use small values for the amplitude of variation of  $B_{1,2}$ , assuming  $K_1 = 0.1$  and  $K_2 = 0.15$ .  $K_1/K_2$  is smaller than the limit expressed by Equation (9). We found that reasonable results are also obtained for even smaller values of modulation (such as  $K_1 = 0.05$ ,  $K_2 = 0.1$ ). The amplitude of observed intensity, however, reduces for smaller values of  $K_{1,2}$ . A phase difference  $\phi$  of the field variation at the two regions is required to produce an observable ( $\Delta t/p$ ). For  $A \cong 1.4$ , and  $K_1 = 0.1$  and  $K_2 = 0.15$ ,  $\tau_0 \approx 0.4$ , we can obtain ( $\Delta t/p$ ) ranging from 0.1 to 0.5 for  $\phi$  ranging from  $120^\circ$ – $180^\circ$ . In Figure 7 we adopted  $\phi = 160^\circ$ .

The plot in Figure 7 is not sensitive for  $A = 1.3$ – $1.5$ . For  $\tau_0 \lesssim 0.1$ , there is no phase difference, and for  $\tau_0 \gg 1.0$ , the phase difference exceeds  $180^\circ$  (or  $\Delta t/p < -0.5$ ). The phase difference observed in the example analysed in this paper ( $\Delta t/p \approx 0.2$ ) is obtained for  $\tau_0 \approx 0.3$ – $0.4$ . Adopting this value of  $\tau_0$  for 22 GHz we can estimate the spectral peak frequency by derivating Equation (5) in relation to  $\nu$ , and using Equations (2), (3), and (7). We determine a peak frequency of about 17 GHz, which is entirely reasonable for this event.

For  $K_1$  changing from 0.05–0.1; we have  $K_2 \approx 0.08$ – $0.2$  in order to get  $\Delta t/p \approx 0.2$ , with the same values adopted for  $A = 1.3$ – $1.5$  and  $\phi = 160^\circ$ .

The consequent changes in the relative amplitude of the observed oscillations,  $\Delta I/I$ , has been determined numerically, using Equation (5) with Equations (2), (3), (4), and (8).  $\Delta I/I$  becomes larger for higher frequencies, which is in agreement with the observations. For example, for  $A \approx 1.4$ ,  $\phi \approx 160^\circ$ ,  $K_1 \approx 0.1$ , and  $K_2 \approx 0.15$ , we obtain 10% of relative amplitude modulation at 22 GHz, and 22% at 44 GHz, which are comparable to the observed relative amplitudes of the oscillation (i.e., 5% at 22 GHz and 20% at 44 GHz).

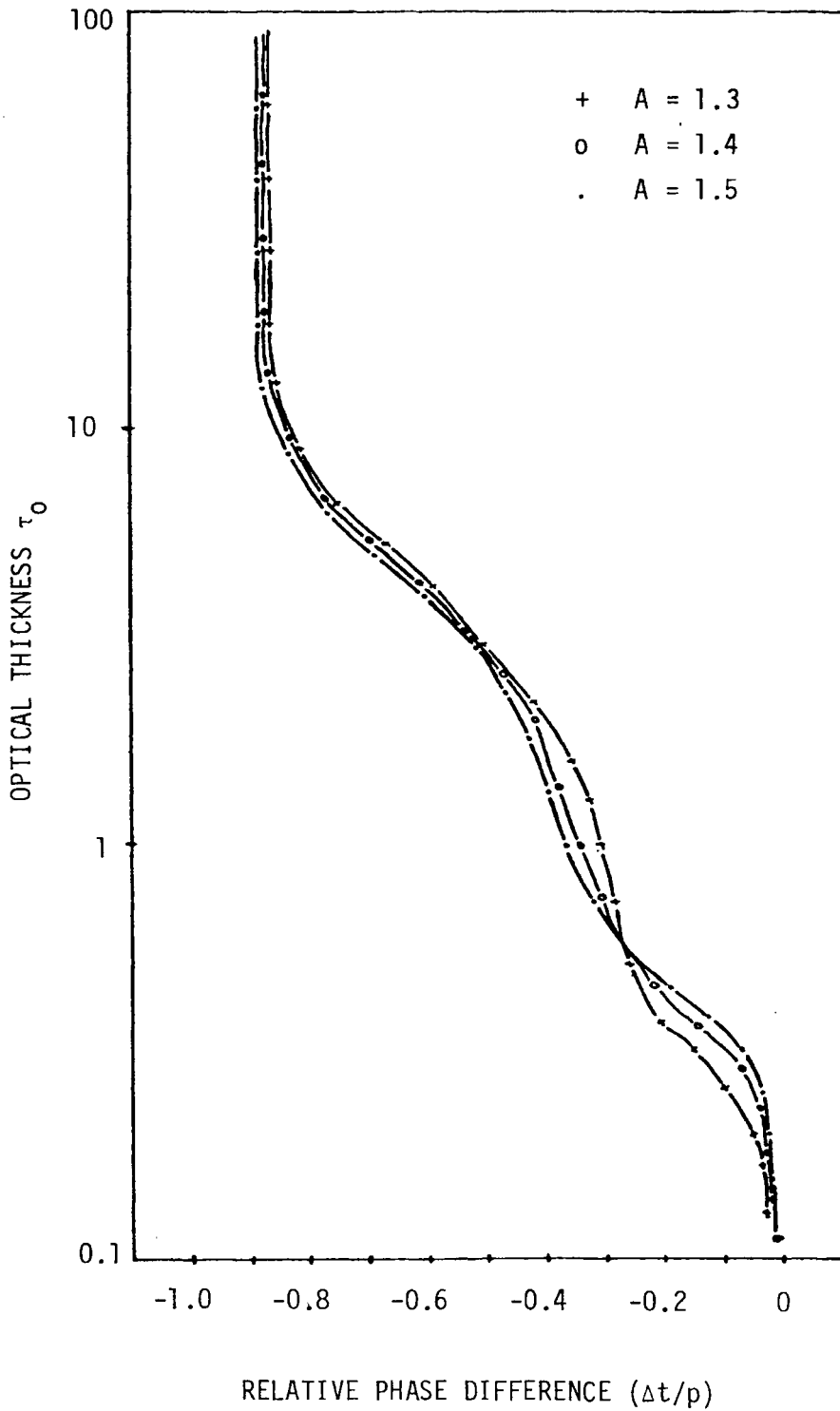


Fig. 7. The dependence of the phase difference (expressed as a fraction of the periodicity ( $\Delta t/p$ )) on the optical thickness, parametric in the ratio of the magnetic field at the two footpoints ( $A = \underline{B}_{01}/B_{02}$ ).

## 7. Final Comments

Persistent 1.5 s quasi-periodic oscillations superimposed to a solar burst were observed at 22 GHz and 44 GHz, with the 44 GHz time structures delayed with respect to the 22 GHz time structures by 0.3 s. The stability of the repetition rate and phase delay over a long duration (about 10 min) suggests that the pulsations are due to a modulation process. We have shown that small variations of the magnetic field on a slightly asymmetrical bipolar loop, are capable to modulate the emitted synchrotron radiation and produce the observed phenomena.

The proposed explanation is the simplest, and is not necessarily unique. As mentioned in the previous section, Tapping (1983) suggested that synchrotron emission can be efficiently modulated by torsional waves, producing persistent and stable periodicity during long durations.

One alternative would be to conceive the quasi-periodic superimposed time structures as modulation of the electron supply or periodic behaviour in a succession of bursts. Kattenberg and Kuperus (1983) observed fast microwave pulsations which were coherent over a distance of the order of  $10^4$  km. They interpreted them in terms of modulation of the electron acceleration process, due to MHD oscillations in a small region above the microwave source. Phase delays of burst time structures at different microwave frequencies have been explained by conceiving each structure as an independent burst and assuming each burst build up by multiple emitting kernels, convoluted in time and space and not resolved in time by instrumentation (Brown *et al.*, 1983). Another explanation assumes a single, or multiple emitting burst sources moving in a loop with a time-varying magnetic field (Costa and Kaufmann, 1983).

The modulation of the radiation by MHD waves is a lower energy process and seems to be more appropriate to produce long enduring oscillations. Bursts showing a steady quasi-period throughout the burst duration appear not to be so common, and a larger number of cases should be investigated at various microwave frequencies, as well as at higher energy ranges. The distinction of purely modulating mechanisms from successive burst production as well as the possible relationship between them are important objectives for further research.

## Acknowledgements

We are grateful to the referee, whose corrections and suggestions have improved the clarity of this paper. We acknowledge Dr G. J. Hurford (CALTECH) in providing OVRO 10.6 GHz interferometer data on this event. We also are grateful for the useful discussions about this research made with H. S. Sawant, J. C. Brown, E. Correia, and J. E. R. Costa. This research was partially supported by Brazilian Research agencies FINEP and FAPESP. INPE operates CRAAM and Itapetinga Radio Observatory.

## References

- Brown, J. C., MacKinnon, A. L., Zodi, A. M., and Kaufmann, P.: 1983, *Astron. Astrophys.* **123**, 10.
- Chiu, Y. T.: 1970, *Solar Phys.* **13**, 420.
- Costa, J. E. R. and Kaufmann, P.: 1983, *Astron. Astrophys.* **119**, 131.
- Emslie, A. G.: 1981, *Astrophys. Letters* **22**, 171.
- Feldman, U., Liggett, M. A., and Zirin, H.: 1983, *Astrophys. J.*, in press.
- Gaizauskas, V. and Tapping, K. F.: 1980, *Astrophys. J.* **241**, 804.
- Gotwols, B.: 1973, *Solar Phys.* **33**, 475.
- Janssens, T. J. and White, K. P.: 1969, *Astrophys. J.* **158**, L127.
- Janssens, T. J., White, K. P., and Broussard, R. M.: 1973, *Solar Phys.* **31**, 207.
- Kattenberg, A. and Kuperus, M.: 1983, *Solar Phys.* **85**, 185.
- Kaufmann, P., Piazza, L. R., and Rafaelli, J. C.: 1977, *Solar Phys.* **54**, 179.
- Kaufmann, P., Strauss, F. M., Opher, R., and Laporte, C.: 1980, *Astron. Astrophys.* **87**, 58.
- Kaufmann, P., Strauss, F. M., Schaal, R. E., and Laporte, C.: 1982a, *Solar Phys.* **78**, 389.
- Kaufmann, P., Costa, J. E. R., and Strauss, F. M.: 1982b, *Solar Phys.* **81**, 159.
- Kaufmann, P., Correia, E., Costa, J. E. R., Dennis, B. R., Hurford, G. J., and Brown, J. C.: 1984, *Solar Phys.* **91**, 359.
- Kosugi, T.: 1981, *Solar Phys.* **71**, 91.
- Kundu, M. R. and Vlahos, L.: 1979, *Astrophys. J.* **232**, 592.
- Maxwell, A. and Fitzwilliam, J.: 1973, *Astrophys. Letters* **13**, 237.
- NOAA: 1981a, *Solar Geophysical Data*, No. 438, Part I.
- NOAA: 1981b, *Solar Geophysical Data*, No. 438, Part II.
- Pacholczyk, A. G.: 1970, *Radio Astrophysics – Nonthermal Processes in Galactic and Extra Galactic Sources*, W. H. Freeman and Company, San Francisco.
- Parks, G. K. and Winckler, J. R.: 1969, *Astrophys. J.* **155**, L117.
- Roberts, B., Edwin, P. M., and Benz, A. O.: 1983, *Nature* **305**, 688.
- Roberts, B., Edwin, P. M., and Benz, A. O.: 1984, *Astrophys. J.*, in press.
- Spruit, H. C.: 1982, *Solar Phys.* **75**, 3.
- Tapping, K. F.: 1978, *Solar Phys.* **59**, 145.
- Tapping, K. F.: 1983, *Solar Phys.* **87**, 177.
- Urpo, S., Tiuri, M., Tlamicha, A., and Pracka, M.: *Astron. Astrophys.* **93**, 121.
- Zirin, H. and Neidig, D.: 1981, *Astrophys. J.* **248**, L45.